Vibration Signal Analysis for the Lifetime-Prediction and Failure Detection of Future Turbofan Components

N. Mokhtari, M. Grzeszkowski, C. Gühmann

Planetary gearbox and hydrodynamic journal bearings (HJB) are going to be integrated in future turbofan engines. This paper presents the results of applied methods to detect failures of these components. At first, failure detection requirements are derived by using system engineering techniques. In consideration of the identified failures theoretical assumptions are discussed and subsequently verified. Vibration and acoustic emission (AE) sensors seem promising to detect failures in an early stage. To prove the theoretical considerations experiments are carried out on test benches.

Tooth flank damage of a planet gear in a planetary gearbox design is investigated. High demands are placed on the signal processing due to design-related amplitude modulation effects. Vibrations are measured using acceleration and AE sensors, which are mounted on the ring gear. The investigated failure type leads to excitation of non-stationary AE signals. It is proposed that the AE signals have a cyclostationary characteristic. Using cyclostationary-based processing techniques the signal's hidden periodicities can be revealed. A separated analysis of each planet and evaluation of the envelope spectrum finally allows the detection of this failure type.

Instead of roller bearings, HJB can be integrated in planet gears. The most essential damaging mechanism for HJB is wear as a result of mixed or boundary friction. These friction states are caused by conditions like Start/Stop Cycles, insufficient oil supply, overload or oil contamination. The accumulated intensity and duration of friction can be a measure of the remaining useful lifetime (RUL). To estimate the RUL friction has to be differentiated regarding the intensity. AE technology is a promising method to detect friction in HJB. Therefore, AE signals of the mentioned conditions are acquired. Due to rotating planet gears there is no possibility to place AE sensors directly on the surface of HJB.

Finally suitable features for both components are extracted from the processed signals. Their separation efficiency with respect to the failure types is evaluated.

1 Introduction

1.1 Planetary Gearbox

Planetary gearboxes are frequently used in applications where high power densities are in great demand, such as wind power plants and helicopter drivetrains. Furthermore, future technologies of geared turbofans in civil aviation will also use a planetary gearbox in the drivetrain to reduce the fans speed and to increase the turbines speed. This leads to an increase of turbine efficiency and a reduction of noise, because the fan and the low-pressure turbine operate in their optimum working point. With the use of a gearbox further maintenance actions are required to ensure a reliable detection of gearbox faults due to wear and gear defects at an early stage. Therefore customers are interested in planning a condition-based maintenance in addition to time scheduled maintenance.

The main fault types in planetary gearboxes are tooth cracks in the dedendum (Reimche et al., 2007; Mohammed and Rantatalo, 2016), tooth break (Yoon et al., 2014) and carrier cracks (Ompusunggu et al., 2014; Blunt and Keller, 2006). To prevent the gearbox from a total failure, cracks and intense wear have to be detected in an early stage. A majority of the faults can be detected by acquiring the gear vibrations or the acoustic emission (AE) of the gearbox components. The disadvantages of these kind of signals are the complex signal structure and modulation effects due to the planet rotations, which lead to high requirements on the diagnostic methods (McFadden and

Smith, 1985). The sensor signatures which are related to a fault case can then only be detected and explored with the use of extensive signal processing methods.

During the gear meshing the time-variant tooth stiffness leads to excitation of acoustic waves in the sun gear, planet gears and the ring gear (Vicuna, 2009). This phenomenon represents the main excitation source for the gearbox vibrations, which can be measured with accelerometers located on the gearbox housing or the ring gear. Furthermore the planets cause an elongation of the ring gear in radial direction. This effect, on the other hand, can be measured using sensors which are sensitive to strain like strain gauges or fiber-optic sensors (Hoffmann et al., 2007).

This contribution presents a method for the diagnosis of planet gear cracks. Due to the rotation of the planet gears, signal processing methods are presented, which estimate the planets position for an efficient feature extraction process. The developed fault detection methods form a possible basis for the development of further techniques for the failure detection in planet bearings.

1.2 Hydrodynamic Journal Bearing

As described roller bearings are used in planetary gearboxes to reduce friction between pins and planets and to allow only the desired direction of movement. Instead of roller bearings, hydrodynamic journal bearings (HJB) can be integrated in planets. For this type of bearing a continuous oil supply is needed. Because of the eccentric position of the pin in the journal bearing and simultaneously relative movement of these components, the oil pressure is in equilibrium with the outer bearing load, so that a supporting oil film is formed. This supporting oil film separates the pins surface and journal bearings surface, so that only fluid friction can occur (Deters, 2014). This condition prevents mixed friction and solid friction, which are not desired. Mixed friction and solid friction cause wear, which is the most essential damaging mechanism for HJB (Albers and Dickerhof, 2010; Albers et al., 2012).

HJBs have many advantages over roller bearings. On the one hand, HJBs are non-sensitive against impact load, high oscillations and vibrations, and on the other hand, they have a simple structure, a very low noise level and are more suitable for high speeds compared to roller bearings. HJBs also have disadvantages. At low speed levels, machine shut down, lack of lubrication, overload or contamination, mixed or solid friction is generated between the journal bearing and pin (Kelm, 2009). Friction, which evokes wear, reduces the lifetime of HJB's and causes fatal failures. To prevent negative impact on product reliability, which causes high maintenance costs and downtime, the HJB's condition has to be known. One possibility to record friction is to use AE Technology. This method promises many advantages in terms of sensitivity to friction and failures compared to normal vibration measurements (Raharjo, 2013; Al-Ghamd and Mba, 2006). With suitable evaluation methods of the acquired AE signal and calculation tools the intensity and duration of mixed friction can be determined. This information can then be used to develop a remaining useful lifetime model.

2 Planetary Gearbox

2.1 Test Bench

The test bench (see Figure 1), which is being used for the planetary gearbox condition diagnosis measurements consists of a drive motor with a nominal torque of 320 Ncm at 3000 rpm. The maximum speed is limited to 3000 rpm. The torque is simulated by a magnetic powder brake with a maxmimum of 1 kW brake power. The driven gearbox consists of one planetary gear unit with a sun gear (50 teeth), three planets (35 teeth) and a fixed ring gear (120 teeth). These are spur-toothed gears with an 20 pressure angle. The planetary gear has a transmission ratio of 3.4 and a module of 1.5.

During tests, the vibration signals from a piezoelectric acceleration sensor mounted on the ring gear were acquired. Additionally, an AE sensor from PZT material (lead zirconate titanate) was mounted on the ring gear front side to measure high frequency AE signals resulting from tooth meshing. Centrifugal forces, which act on the ring gear when a planet gear passes the sensor, lead to low-frequency radial strain of the ring gear which is also acquired with the AE sensor. The sensor signals from a tachometer and a torquemeter installed on the output shaft were also
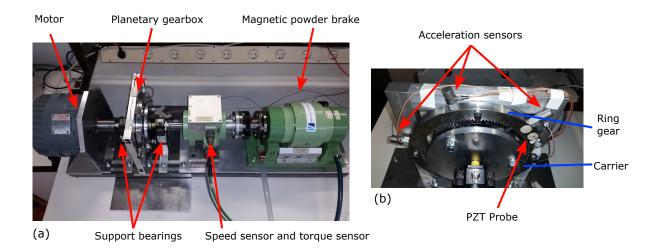
Figure 1: Planetary gearbox subscale test rig: (a) Motor-powered test bench, (b) Applied sensors at the planetary gearbox

acquired. The mentioned signals were sampled with a sampling frequency of 50 kHz to an extent of about 140 revolutions of the carrier.

2.2 Experimental Procedure

The proposed test campaign tests were carried out at different conditions of failure, driving speed and applied torque. The defined gearbox tests are listed in Table 1. To simulate a faulty gearbox a tooth crack with different crack depths at one definied planet gear were artificially inserted. The damage was inserted at the tooth root area at an angle of 30 related to the normal of tooth crest. A damaged tooth with the deepest crack is shown in Figure 2. As shown in Table 1, 45 test-runs were performed for every gearbox, whereas two gearboxes initially in a good condition were used in this test campaign.

Figure 2: Artificially cracked planet tooth

Table 1: Overview of the PG experiments

Parameter	Range
Sun speed	300 rpm, 512 rpm, 670 rpm
Torque	0 Ncm, 250 Ncm, 500 Ncm
Condition	Gearbox in good condition, 0.4 mm crack, 0.8 mm crack, 1.2 mm crack, 2.4 mm crack
Fault type	Artifical planet gear crack

2.3 Signal Processing Methods

To extract features for gear state estimations, two different kinds of features are investigated: Global features, which are calculated over the total carrier revolution and local features, derived from time windowed vibration signals, corresponding to specific gear teeth being in contact. The applied signal processing techniques are summarized in Figure 3.

Firstly, the vibration sensor signals and AE sensor signals were resampled using the speed sensor signal for every test-run with specific speed, torque and crack depth. The resampling process is used to reduce a smearing of the spectral lines in the FFT spectrum, which arise from speed fluctuations of the motor. Resampling is also required for the following order analysis, where speed-independent feature-carrying sidebands are gathered for the feature extraction process. Here especially the meshing order sidebands are recovered and extracted for further calculations, because of the impact a cracked planet tooth has on the amplitude modulation process (Shan et al., 1999).
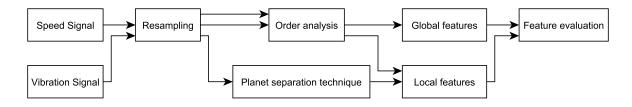

Figure 3: Signal processing

2.3.1 Planet-Separation

In previous investigations (McFadden and Smith, 1985) it could be observed that the level of the measured vibrations reaches a peak value when the planet is closest to the acceleration sensor. As a result of this observations McFadden (McFadden, 1991) developed a method to average the vibration signals of the individual planet gears and the sun gear through windowing the time period, where a planet passes the acceleration sensor. The idea of this method is integrated in this work, to enhance the sensitivity of features to planet cracks.

To use this differential planet diagnosis method through windowing the time signals, the teeth on the planet gear should be meshing with the same teeth on the ring gear near the sensor for every considered window. This state of the appropriate kinematic values is reached periodically every N_c carrier revolutions forming a period length of $T_p = N_c \cdot T_c$, where T_c is the period of one carrier revolution. Therefore, a synchronization of the vibration signals between the test-runs was realized. The sensor signals were synchronized through correlation analysis between the vibration signals of two different test-runs with same speed and torque but different gear failure conditions. This calculation is possible, because of the unequal planet load sharing due to manufacturing and assembling errors. Afterwards the signals are averaged over one state period T_p, to separate the vibration signature of the individual fixed-axis gears from the total vibration of the gearbox.

After the synchronization process the center point of the window functions, where one planet is closest to the sensor, has to be defined. For this purpose the displacement sensor signal from the PZT probe (see Figure 1b) is evaluated. The displacement sensor acquires the radial strain on the ring gear when the planets pass the displacement sensor. Investigations showed, that this sensor is more sensitive to radial strain through planet passing, than the acceleration sensors mounted on the ring gear's circumferential side.

With the processed displacement signal the equally spaced center points of the window function $w(t)$ can be gathered and multiplied with the vibration sensor signal $x(t)$ (see Figure 4). The resulting sensor signals $x_w(t, n)$ correspond to the vibrations at specific meshing points between teeth on the planet gears and teeth on the ring gear (Elia et al., 2013):

$$x_w(t,n) = x(t) \cdot w\left(t - n \cdot \frac{T_c}{N_p}\right) . \tag{1}$$
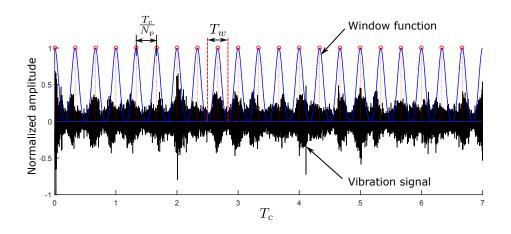
Figure 4: Windowed vibration signal

The value N_p represents the number of planets. The window width T_w has to be chosen appropriately to include all planet tooths of interest on one hand, and on the other to ensure an isolated planet tooth crack detection. It could be claimed that with rising state period T_p a smaller window size can be used. Afterwards local features can be extracted from the windowed sensor signals.

2.4 Results and Interpretation

An evaluation of the extracted global features root mean square (RMS), crest factor, peak value, standard deviation, skewness, kurtosis and the zero-order figure of merit parameter (FM0) (Vecer et al., 2005) showed, that there are no exploitable global features which correlate with the depth of the planet tooth crack. Only the feature FM0 showed negligible increased values with increasing crack depth at 670 rpm sun gear speed and a load of 500 Ncm.

The local features were calculated within every windowed time signal for the 3 planet gears. To find the correlations between specific feature values and the gearbox fault conditions the covariance matrices of the planet-specific features were calculated for a given motor speed and load. In Figure 5 two features (peak value and FM0-value) are shown for measurements at 300 rpm sun gear speed which seems to correlate with an increasing tooth crack depth.

To understand the relations between the feature values and the crack propagation further investigations have to be done in future work to finally estimate the gearbox condition. Because the time windowed extraction of local features seems to be a promising method, the condition of every single tooth pair should be monitored speed- and torque-independent by means of AE signal analysis. Therefore tooth meshing patterns generated from AE measurements will be analyzed using methods of classification. The methods should enable a discrimination between different time-windowed tooth meshing pairs utilizing manufacturing and assembling errors. This would allow the assignment of time-windowed features from same tooth meshing pairs of different measurements.
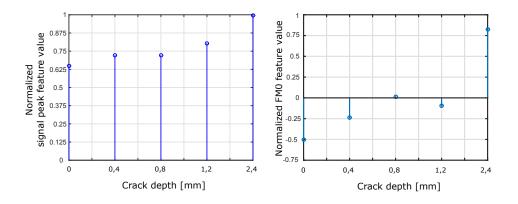

Figure 5: Feature values for measurements at 300 rpm sun gear speed

3 Hydrodynamic Journal Bearing

3.1 AE Technology

AEs are elastic waves that are generated by suddenly released elastic energy e.g. due to material deformation or damage. In addition, friction also generates AE, which is then transferred within the material or on the surface and can be detected by a sensor. From the molecular lattice theory point of view, AEs are generated as follows (Huang et al., 2007): If two surfaces rub against each other the molecule moves from a stable lower state to an unstable upper state. The energy generated during this process accumulates until a maximum is reached. After reaching this state, the molecule slips to the adjacent lower state to reach a new stable state. In this dislocation and slip process the molecule releases energy. One part of the strain energy propagates from the internal to the surface in form of elastic stress waves. The frequency ranges between infrasonic and ultrasonic range (typically between 30kHz - 2MHz). An AE sensor consists of a PZT, which works at its resonance frequency range to reach maximum sensitivity.

3.2 Subscale Journal Bearing Test Rig

Figure 6 shows the journal bearing test rig at which all tests were carried out. A Mattke servomotor drives the shaft. Two supporting roller bearings are located at the left and right side of the journal bearing. Two nylon strips are applied between the shaft and the supporting bearings to mostly reduce interfering signals. A Festo pneumatic cylinder provides the load for the journal bearing. The journal bearing consists of a bearing bush, which is made of the actual bearing material and a bearing back to prevent dilatation. The bearing back is made of two parts, which can be fixed with screws, to replace the journal bearing easily. A gear pump transports oil through a drilling, which is located on the lower part of the bearing back.
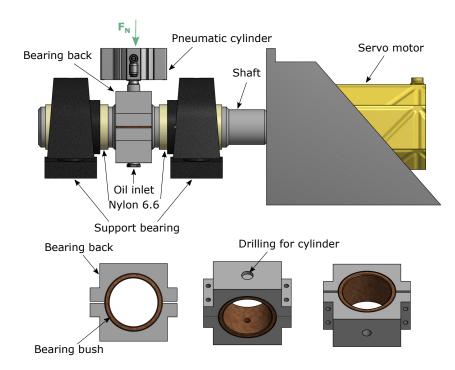

Figure 6: Journal bearing test rig

A PAC (physical acoustics cooperation) Wideband AE sensor with a frequency range of 100-900 kHz is mounted on the upper part of the bearing back next to the drilling for the cylinder. A 2/4/6 preamplifier is used to amplify and filter the AE signals. The oil temperature influences the oil viscosity, which again influences the AE signal. For this reason, the oil temperature needs to be held as constant as possible. A Pt100 sensor measures the oil temperature. A pressure transducer is used to measure the oil inlet pressure. The sensor signals are sampled at 200 kHz. Table 2 shows the test conditions at the test rig.

Table 2: Overview of the test conditions at the HJB test rig

Bearing bush diameter	50 mm
Bearing bush width	40 mm
Maximum speed	3000 rpm
Maximum load	3 kN
Oil inlet temperature	Constant at 27 °C
Oil inlet pressure	Constant at 2 bar
Oil	Hydraulic oil ISO VG 10
Bearing bush material	Red bronze
Shaft material	ST52-3

3.3 Test Description: Static hydrodynamic Friction and mixed Friction Conditions

This section describes the driven tests and their advantages for the detection of friction. At constant load and decreasing speed the gap between HJB and shaft also decreases, which ultimately results in mixed friction at lower deviation of the narrowest gap h_0. As already described this condition should be avoided during operation because it affects the lifetime of the HJB negatively and can cause failures if it is repeated. Mixed friction is caused deliberately by decreasing the speed at constant load and oil viscosity with purpose of detecting mixed friction conditions in normal operation in the future.

With suitable evaluation methods, the border between fluid friction and mixed friction should be identified. For this purpose the Stribeck curve is used, which shows the relationship between speed, load and viscosity with the coefficient of friction. The sensor data in fluid friction condition could be used as a reference data for the safe condition of the HJB.

3.4 Results and Interpretation

Figure 7 shows the AE RMS plotted against the speed at a constant load of 1750 N. The speed was decreased from 350 rpm up to 60 rpm with 10 rpm steps. The trend shows a high AE RMS value at low speeds, which decreases with increasing speed until a minimum is reached. From this minimum the AE RMS increases again. To understand this trend the knowledge about the Stribeck curve is needed.
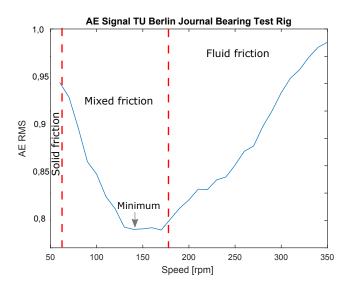

Figure 7: HJB hydrodynamic and mixed friction test; AE RMS at a load of 1750 N

The Stribeck curve indicates the relationship between the viscosity, speed and load with the coefficient of friction. At low viscosity or low speed or at high load the coefficient of friction increases. If the viscosity or speed increases or the load decreases then the gap between the shaft and HJB increases and the oil film becomes thicker. If the speed

428

continues increasing then the coefficient of friction increases again due to the shear stress of the fluid (Mirhadizadeh et al., 2010). The shear stress results in friction between the fluid and the shaft. This type of friction is not responsible for the wear, which is generated during friction between solid surfaces. Figure 8 (a) shows the Stribeck curve and its friction areas.
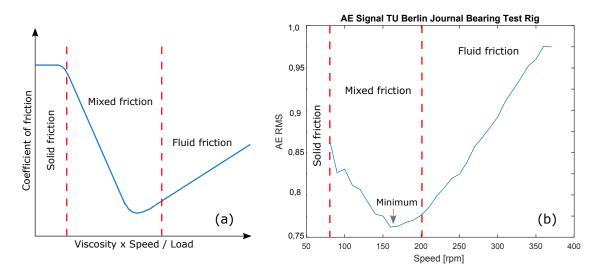

Figure 8: (a) Stribeck curve, (b) HJB hydrodynamic and mixed friction test; AE RMS at a load of 2250 N

With the knowledge about the Stribeck curve, the acquired AE RMS signal can be interpreted. Because the load and the viscosity were held constant, there is only a speed dependency. In the area with low speed and high AE RMS value solid friction occurs. The solid friction area is hardly dependent on the speed. Because of that it seems, that this area could not be recorded (motor stops at high loads). The sensor signals begin at the mixed friction area. At a speed of about 145 rpm the minimum value of AE RMS is reached. The border between fluid friction and mixed friction has not been reached yet because the real minimum oil gap is a subtraction between the theoretical oil film gap and the sum of the shafts and journals roughness. Mixed friction area ends at a speed value of ca. 175 rpm. With higher speed fluid friction begins and the AE RMS signal increases again. In this area there is no asperity contact between shaft and bearing, therefore mixed friction can not occur. Rather the shear stress of the fluid becomes important. The shear stress of the fluid generates friction between the fluid and the shaft and is responsible for the increasing of the AE RMS value. This kind of friction has theoretically no lifetime-reducing effect on the HJB. Concluding it is assumed that a higher shaft speed leads to a higher shear stress and consequently a larger AE RMS value.

The result of a second test with a constant load of 2250 N is shwon in figure 8 (b). It shows a qualitatively similar trend. However, the AE RMS signals minimum is moved a little bit to the right side as expected. The minimum is reached at a speed value of ca. 155 rpm. The reason is that the journal bearing stays longer in mixed friction condition due to the higher load. The duration of mixed friction condition is longer at higher loads. Mixed friction area ends at a speed value of ca. 200 rpm.

4 Conclusion

The presented differential planet processing method, which was used within this work to detect a planet gear tooth crack on a planetary gearbox, shows that the fault detection can be improved, through windowing the time period, where a planet passes the acceleration sensor. The results demonstrate that an accurate planet position estimation can be realized by measuring the ring gear elongation with a PZT probe. In further works the planet separation processing method should be used for the development of a planetary gearbox condition monitoring system.

The tests performed at the HJB test bench show that it is possible to find mixed friction events with AE technology and suitable analysis tools. Furthermore it is possible to differentiate between mild and strong friction. This result can be used for further investigations especially for the calculation of the remaining useful lifetime of a HJB.

References

Al-Ghamd, A. M.; Mba, D.: A comparative experimental study on the use of acoustic emission and vibration analysis for bearing defect identification and estimation of defect size. *Mechanical Systems and Signal Processing*, 20, 7, (2006), 1537–1571.

Albers, A.; Dickerhof, M., eds.: *Simultaneous Monitoring of Rolling-Element and Journal Bearings Using Analysis of Structure-Born Ultrasound Acoustic Emissions*, International Mechanical Engineering Congress & Exposition (2010).

Albers, A.; Nguyen, H. T.; Burger, W.: Energy-efficient hydrodynamic journal bearings by means of condition monitoring and lubrication flow control. *International Journal of Condition Monitoring*, 2, 1, (2012), 18–21.

Blunt, D. M.; Keller, J. A.: Detection of a fatigue crack in a uh-60a planet gear carrier using vibration analysis. *Mechanical Systems and Signal Processing*, 20, 8, (2006), 2095–2111.

Deters, L.: *Dubbel - 5 Gleitlagerungen: Plain bearings*. 24 edn. (2014).

Elia, G. D.; Mucchi, E.; Dalpiaz, G.: On the time synchronous average in planetary gearboxes. In: *International Conference Surveillance 7* (2013).

Hoffmann, L.; Müller, M. S.; Sommavilla, M.; Koch, A. W.: Wälzlagerüberwachung mit faseroptischer sensorik. *tm – Technisches Messen*, 74, 4, (2007), 204–210.

Huang, Q.; Li, L.-p.; Rao, H.-d.; Jin, F.-h.; Tang, Y.-q., eds.: *The AE Law of Sliding Bearings in Rotating Machinery and its Application in Fault Diagnosis*, Hangzhou, China (2007).

Kelm, R. D.: Journal bearing analysis. pages 221–240.

McFadden, P. D.: A technique for calculating the time domain averages of the vibration of the individual planet gears and the sun gear in an epicyclic gearbox. *Journal of Sound and Vibration*, 144, 1, (1991), 163–172.

McFadden, P. D.; Smith, J. D.: An explanation for the asymmetry of the modulation sidebands about the tooth meshing frequency in epicyclic gear vibration. *Proceedings of the Institution of Mechanical Engineers, Part C: Journal of Mechanical Engineering Science*, 199, 1, (1985), 65–70.

Mirhadizadeh, S. A.; Moncholi, E. P.; Mba, D.: Influence of operational variables in a hydrodynamic bearing on the generation of acoustic emission. *Tribology International*, 43, 9, (2010), 1760–1767.

Mohammed, O. D.; Rantatalo, M.: Dynamic response and time-frequency analysis for gear tooth crack detection. *Mechanical Systems and Signal Processing*, 66-67, (2016), 612–624.

Ompusunggu, A.; Y'Ebondo, B.; Devos, S.; Petre, F.: Towards an automatic diagnostics system for gearboxes based on vibration measurements. *International Conference on Noise and Vibration Engineering (ISMA)*, 26, (2014), 2849–2863.

Raharjo, P.: *An Investigation of Surface Vibration, Airborne Sound and Acoustic Emission Characteristics of a Journal Bearing for Early Fault Detection and Diagnosis*. Dissertation, University of Huddersfield (2013).

Reimche, W.; Scheer, C.; Bach, F.-W.: Frühzeitige schadenserkennung an rotierenden bauteilen mittels schallemissionsanalyse und einer wirbelstromtechnik unter anwendung der wavelet-transformation. *Schwingungsüberwachung und Diagnose von Maschinen VDI-Berichte Vol. 1982, S. 39-55. Düsseldorf: VDI-Verl., 2007*.

Shan, J.; Bauer, B.; Seeliger, A.: Schadensdiagnose von planetengetrieben mit hilfe der schwin- gungsanalyse. In: *Schwingungsüberwachung und -diagnose von Maschinen und Anlagen*, VDI-Berichte, VDI-Verl., Düsseldorf (1999).

Vecer, P.; Kreidl, M.; Smid, R.: Condition indicators for gearbox condition monitoring systems. *Acta Polytechnica*, Vol. 45 No. 6, (2005), 1–6.

Vicuna, C. M.: *Contributions to the analysis of vibrations and acoustic emissions for the condition monitoring of epicyclic gearboxes*. Dissertation, RWTH Aachen, Aachen (2009).

Yoon, J.; He, D.; Van Hecke, B.; J. Nostrand, T.; Zhu, J.; Bechhoefer, E.: Planetary gearbox fault diagnosis using a single piezoelectric strain sensor. *ANNUAL CONFERENCE OF THE PROGNOSTICS AND HEALTH MANAGEMENT SOCIETY 2014*, 5, (2014), 118–127.

Address: Technische Universität Berlin
School of Electrical Engineering and Computer Science
Department of Energy and Automation Technology
Chair of Electronic Measurement and Diagnostic Technology
Sekretariat EN13
Einsteinufer 17 - 10587 Berlin

email: noushin.mokhtari@tu-berlin.de
mateusz.grzeszkowski@tu-berlin.de
clemens.guehmann@tu-berlin.de